EVALUATION OF MAGNETIC FIELD ENHANCEMENT ALONG A BOUNDARY

Y. Iwashita, ICR, Kyoto Univ., Kyoto, JAPAN
T. Higo, KEK, Tsukuba, JAPAN

Abstract

Only the high electric field gradient on boundaries has been thought to cause sparking in a cavity, and designers have been taking much attention on avoiding sharp edges in such an area to reduce peak electric field gradient. Recently, not only the electric field but also magnetic field on an edge can cause the spark problem through heating up of the very local surface material by concentration of the magnetic field density. The effects were numerically evaluated through a simplified model.

INTRODUCTION

There are three requirements for the accelerator structure of the main linac of the linear collider GLC/NLC[1]:

1) high gradient (50MV/m),
2) suppression of wake field and
3) low cost in mass production.

The first two items are of concern in the present paper. The second requirement was proved to be met by the DDS (Damped Detuned Structure) that can suppress the long wake field [2]. In order to meet the first requirement, the design parameters have been evolved for a few years to date to adopt low group velocity and high phase advance features [3]. The resultant recent shape of the relevant constituent disk is shown in Fig. 1.

It was known that the magnetic field that crosses a ridge-like geometry was enhanced at the ridge. The enhanced field results in a huge temperature rise within a pulse (see Fig. 2). Typical example was described in [4] where copper surface with low electric field but high magnetic field was cracked and/or eroded identified after numerous number of breakdowns near the ridge. Considering these, we designed and fabricated the HDDS disks, which does not have any area where severe magnetic field enhancement did not appear. In the present paper are described the enhancement characteristics relevant to this HDDS disks. Understanding the sensitivities on relevant parameters and proper tolerance setting is very important to pursue the structure mass production stably in an inexpensive manner.

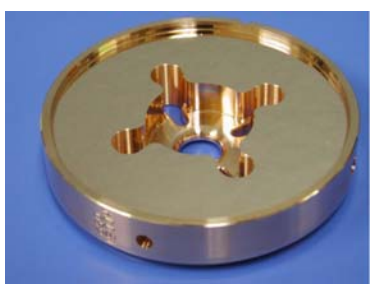

Figure 1: The HDDS cell.

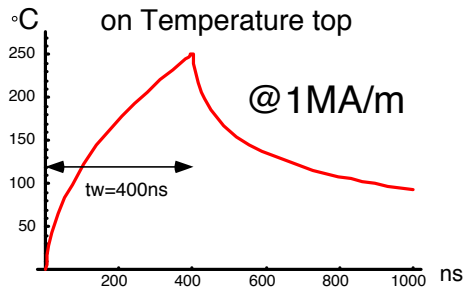

Figure 2: Pulse temperature rise on a flat copper surface where the pulse surface current is 1MA/m and the duration is 400ns. The temperature value should be scaled with the square of the surface current. A reference value of a surface current for a 2D cell without a local enhancement is 0.2MA/m, which reaches 1MA/m when the enhancement factor at a convex corner is 5. This temperature rise becomes more at a convex corner, where a heat capacity is less.

SURFACE CONFIGURATION

As seen in Fig. 3, there are two areas, shown in red, where magnetic field is naturally large. The first is the opening from accelerator cell to HOM manifold. The second is located at each slot, which is needed to extract HOM dipole filed to manifold. From these features, the enhancement at these two areas is inevitable. We evaluated on these geometries.

The assumed geometry is a parallel cut into the outer diameter of a pillbox. The width of the opening and the edge angle are the important parameters. The very edge of the opening is assumed to be rounded by 5 microns reflecting to the fact that these disks are chemically etched by about 3 microns in the fabrication stage so that the similar amount of rounding, 5-micron radius, is assumed at the very edge.

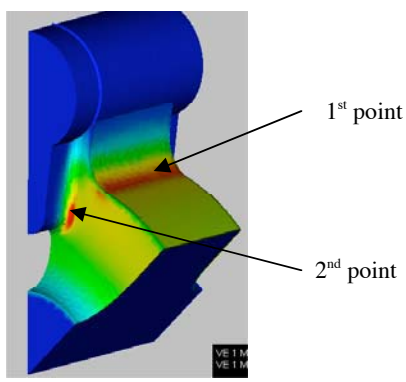

Figure 3: Magnetic field distribution on the surface.

SIMULATION

Although the objects to be evaluated have 3D boundaries, we need a simple model to extract the characteristics. A cylindrical cavity with two waveguide ports is considered in 2D and the problem region is reduced to one quarter because of the symmetries in horizontal and vertical directions (see Fig. 4). Axisymmetric modes TM_{010} in the cylindrical cavities are analyzed as Eigenvalue problems with Finite Element Method. The convex edge with the crossing angle X between the two-machined surfaces (lathed surface with radius R11 and milled surface with radius r) is assumed to be rounded to with 5-μm radius by an etching rinse. Consequently, there are only round corners and concave edges on the boundary. In order for us to ignore the presence of the bottom (a short plane) for any cases, the waveguide depth is set to twice of its width, which is well below the cut off wavelength.

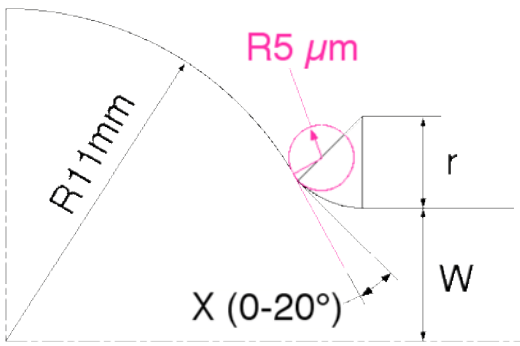

Figure 4: Simplified model for the field enhancement factor.

The problem is analyzed by PISCES-II [5], which uses second order isoparametric finite elements. Because a very fine mesh that can express 5μm radius boundary in 11mm radius area, has more than thousand times ratio in mesh size, a new mesh generator that uses Delauny triangulation [6] is prepared. It generates smooth mesh

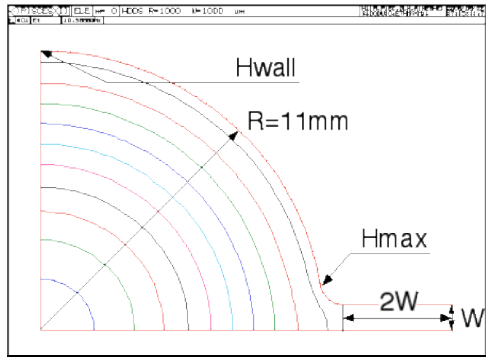

Figure 6: Contour plot of Ez represents magnetic field lines. The enhancement factor is defined by Hmax/Hwall.

where the ratios of the elements sizes between the adjacent elements are less than two (see Fig. 5). The input file format has the same format as that of POISSON/SUPERFISH rel.4.12 for the compatibility.

The magnetic field enhancement factor is defined as the ratio of the fields between two locations Hmax/Hwall: the maximum magnetic field (usually appears at the sharpest curve boundary) Hmax and the magnetic field Hwall at the farthest point from the waveguide (the top of the region). Fig. 6 shows the locations. The Eigenfrequency varies with the parameters while the cavity cell radius is fixed as 11mm. This effect is ignored because it is not serious to the evaluation of the enhancement factor.

PISCES-II can evaluate all Eigenmodes in an axisymmetric boundary including dipole mode (SUPERFISH can obtain only TM0 modes). In order to evaluate the problems described above, capability to analyze in the Cartesian coordinates is added before the series of calculations.

The boundary considered here does not have a convex corner that causes an electromagnetic singular point; the boundary lines and arcs are smoothly connected. The isoparametric second order elements (used in PISCES-II) can express such curved boundaries appropriately and the evaluation becomes accurate.

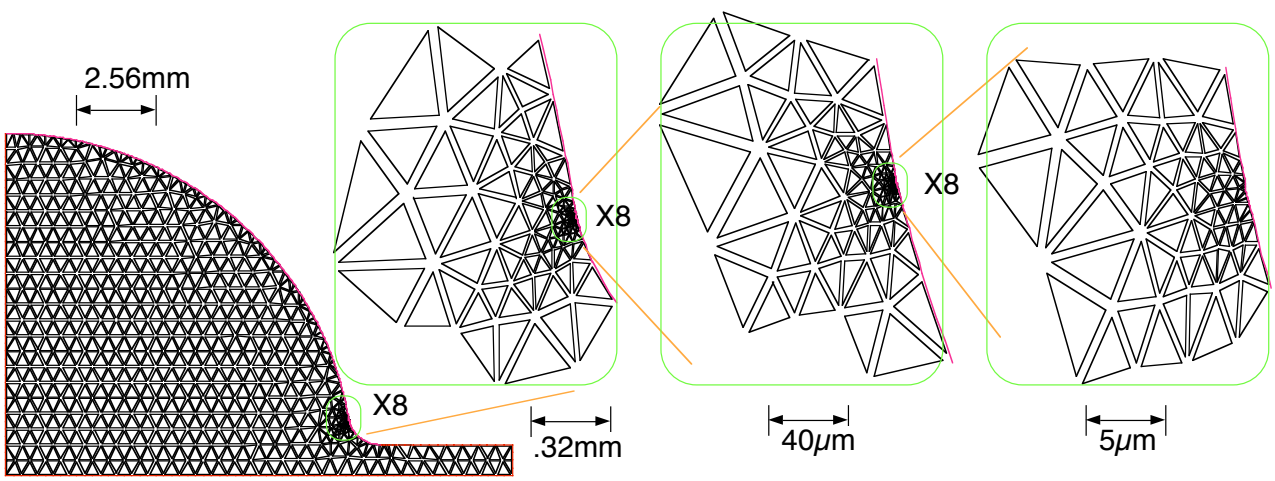

Figure 5: Example of generated mesh with large ratio in mesh size.

RESULTS AND DISCUSSION

The effects on three parameters (W, r and X in Fig. 4) are investigated, where the ranges of the parameters are listed in Table I. The first and the second points in Fig. 3 correspond to (W=3mm, X<5°, r=2mm) and (W=1mm, X~8°, r=0.5mm), respectively. A typical curve for the enhancement factor along the boundary is shown in Fig. 7. The boundary consists of smoothly connected three arcs and straight lines: a concave arc with radius 11mm, a convex 5μm arc and a convex arc with radius r.

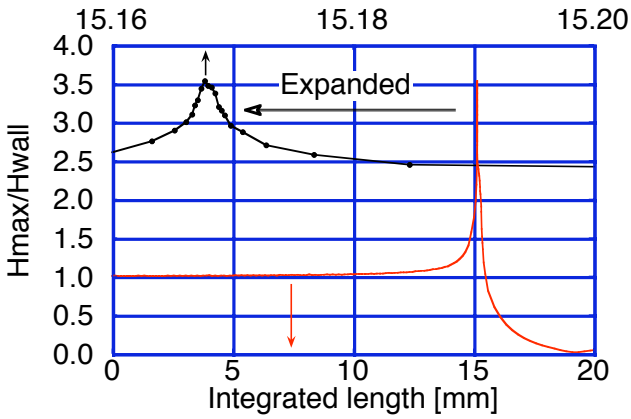

Figure 7: Field enhancement factor along the boundary corresponding to (W=2mm, X=20°, r=200μm). The abscissa shows the integrated distance from the top point where H_{wall} is referred.

Table 1: Input parameters

Half port width	W mm	1, 2, 3, 5
Crossing angle	X degree	0, 5, 12, 20
Radius of opening port	R mm	0.2, 0.5, 1

The enhancement factors for X=0° as functions of r are shown in Fig. 8, where they show $r^{-1/3} \sim r^{-1/4}$ dependences. In order to keep the reproducible connection between the two major arcs in fabrication, a finite crossing angle is needed [7]. The enhancement factors at W=5mm are shown in Fig. 9. This shows the dependencies of power function and the effect of finite crossing angle is prominent when the curvature is small. Fig. 10 shows the dependencies on the crossing angle and the slot width. Three tendencies are shown from the results: 1. the larger the slot width, the higher the enhancement factor, 2. large r reduces the enhancement, 3. large crossing angle decreases the above reduction effect.

In the current cell geometries, the enhancement factors that correspond to the first and second points in Fig. 3, are about 1.5 when the crossing angle is 0°. Although the enhancement factors increase with the finite crossing angles, they can be kept below 2 for the first point if X=5° with W=3 and for the second point if X=8° with W=1 case. From these results, we conclude that practical design is possible for the real cavity cells.

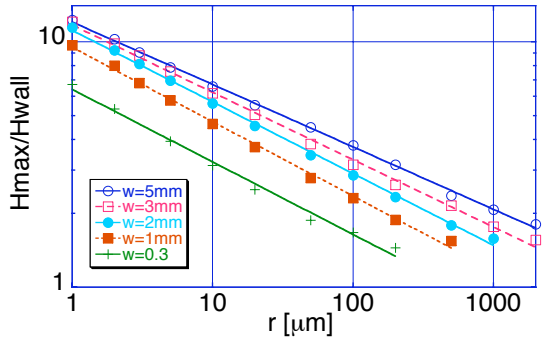

Figure 8: Enhancement factors as functions of r: X=0.

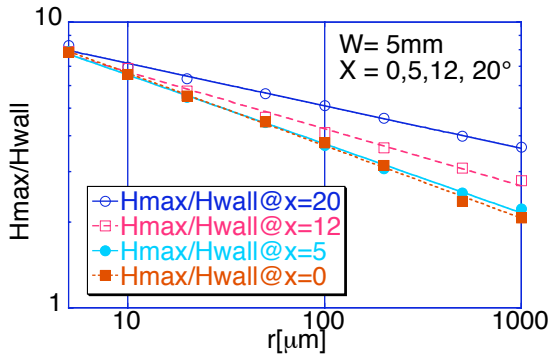

Figure 9: Enhancement factors at finite crossing angles.

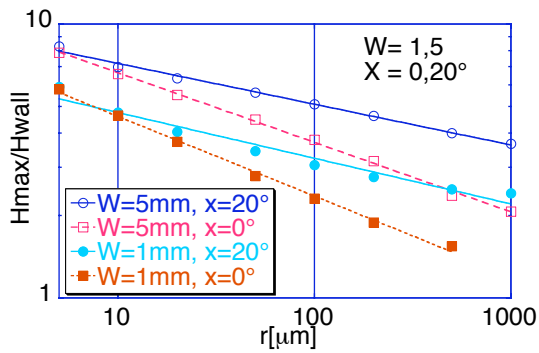

Figure 10: Enhancement factors at finite crossing angles.

REFERENCES

[1] GLC: KEK Report 2003-7, 2003 and http://lcdev.kek.jp/ProjReport/, 2003 and NLC: SLAC Report 474, 1996.
[2] KEK Report 2000-7, SLAC-R-559, April 2000.
[3] J.W. Wang et al.: "Recent progress in R&D of Advanced Room Temperature Accelerator Structures", TH464, Proc. of LINAC2002, Gyeongju, Korea, 2002.
[4] V. Dolgashev, KEK-SLAC ISG9 Meeting, Dec. 2002 at KEK, http://lcdev.kek.jp/ISG/ISG9.html
[5] Y. Iwashita: "PISCESII: 2.5D RF Cavity Code with High Accuracy", Beam Science and Technology, ICR Kyoto Univ., **7**, 14-18 ISSN 1342-033X (2002)
[6] T. Taniguchi: Morikita Shuppan Co. Ltd., ISBN: 627914008, 1992 in Japanese.
[7] T. Higo et al.: "Improved HDDS cell fabrication", GLCX-006, http://lcdev.kek.jp/TechNotes/, 2003